ASME Journal of Engineering and Science in Medical Diagnostics and Therapy
Online journal at:
https://asmedigitalcollection.asme.org/medicaldiagnostics

Data-Driven Depiction of Aging Related Physiological Volume Shrinkage in Brain White Matter: An Image Processing Based Three-Dimensional Micromechanical Model

Mohit Agarwal
Department of Mechanical and Aerospace Engineering Rutgers, The State University of New Jersey, Piscataway, NJ 08854

John Georgiadis
Department of Biomedical Engineering, Illinois Institute of Technology, Chicago, IL 60616

Assimina A. Pelegri
Department of Mechanical and Aerospace Engineering Rutgers, The State University of New Jersey, Piscataway, NJ 08854-8058

Aging in the human brain, both in healthy and pathological conditions, leads to significant microstructural alterations, resulting in cognitive decline, with cerebral atrophy being a major contributing factor. This atrophy, characterized by the loss of neurons and glial cells, plays a crucial role in the reduction of brain function. While magnetic resonance imaging (MRI) and magnetic resonance elastography (MRE) provide noninvasive tools to measure brain morphology (volume changes) and regional mechanical properties (tissue stiffness) at the millimeter scale, they are unable to capture cellular-level or micron-scale changes in brain tissue. The challenge is in correlating the mechanical property changes observed at the millimeter scale with the underlying cellular-level micro-architectural alterations. To address this limitation, an ensemble of three-dimensional micromechanical finite element (FE) models was developed, utilizing MRI/MRE data to compute the mechanics of the aging brain with a higher level of detail. Using image processing techniques in Python's NIBABEL library, a mathematical model was constructed to quantify volume fraction (VF) shrinkage in brain white matter (BWM). These models incorporate uniaxial tensile loading and simulate the interactions between axons, myelin, and the glial matrix. Among the three finite element models compared, model type III, which includes both volume fraction changes and shear modulus degeneration, showed a high-order age-related atrophy and brain softening. This approach emphasizes the significant role of computational mechanics in linking macroscopic MRI measurements to cellular-scale changes, enhancing our understanding of brain tissue degeneration. [DOI: 10.1115/1.4067393]

Keywords: micromechanics, aging, brain, image processing, MRE/MRI, neuroimaging, mathematical modeling, statistics, biomarkers, CNS mechanics, python

1 Introduction

The human brain experiences considerable atrophy, or volume loss, as we age (see Fig. 1). Quantitative evaluation of brain atrophy is essential for monitoring clinical outcomes and treatment efficacy in various diseases, including Alzheimer's disease, multiple sclerosis, schizophrenia, alcoholism, and acquired immunodeficiency syndrome-related dementia. Age-related changes of the human brain, with or without pathology, are also linked to significant alterations in brain tissue microstructure. Even in the absence of disease, (healthy) aging results in regional losses or alterations of neurons and glia cells. The alterations correspond to the loss of dendritic connections in gray matter and neuroinflammation-induced demyelination, axonal death, astrogliosis, and microgliosis in white matter (Fig. 1) [4]. Progressive microstructural degeneration in brain white matter (BWM) leads to tissue softening, shrinkage, and damage. Since these changes are associated with cognitive or motor deficits, or changes in behavior, they provide useful markers for monitoring the onset or progress of brain disease.

Advancements in magnetic resonance imaging and computer technology have enabled the in vivo study of brain morphometrics, allowing for precise, reproducible, and quantitative measurements of brain atrophy and degradation in the aging brain's structural features [5]. Magnetic resonance elastography (MRE) and magnetic resonance imaging (MRI) methods have facilitated noninvasive measurements of changing brain morphology, such as volume and micro-architecture, and have allowed characterization of the brain's

Contributed by the Materials Division of ASME for publication in the Journal of Engineering and Science in Medical Diagnostics and Therapy. Manuscript received August 9, 2024; final manuscript received December 5, 2024; published online January 23, 2025. Assoc. Editor: Mohammad Al-Rawi.

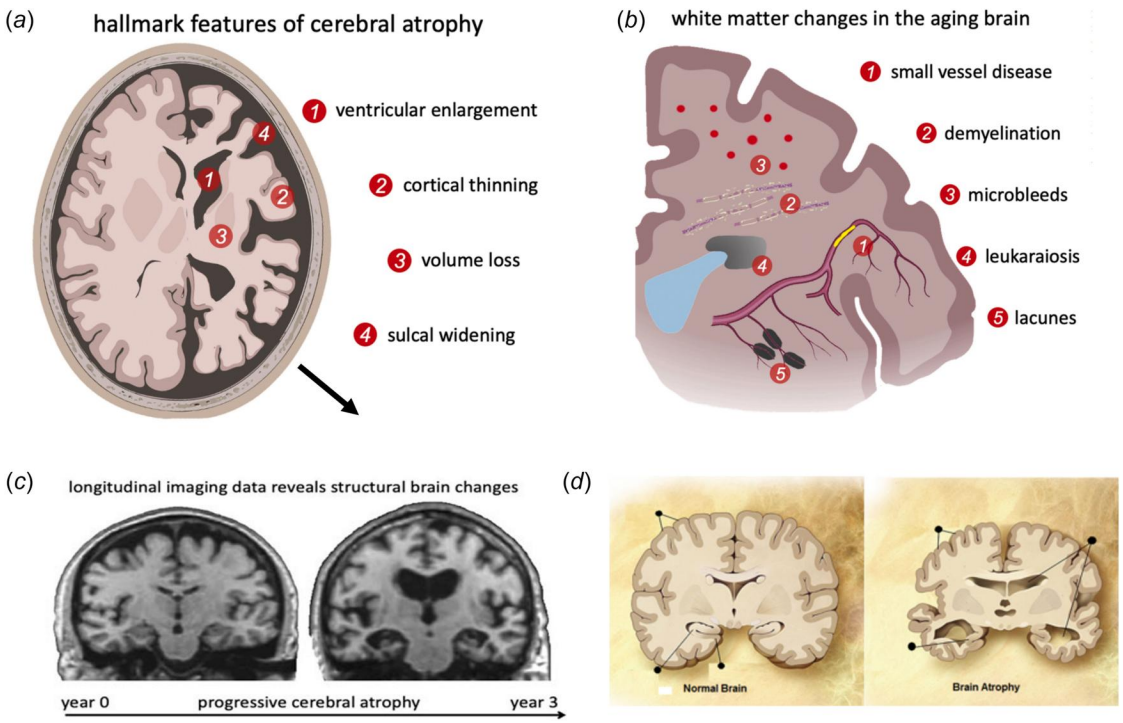

Fig. 1 (*a*) Schematic figure of cerebral atrophy adapted from Blinkouskaya et al. [1] depicting white and gray matter volume loss, cortical thinning, sulcal widening, and ventricular enlargement, (*b*) white matter changes leading to neurodegeneration, adapted from [1], (*c*) two coronal slice images of a subject with severe Alzheimer's disease, highlighting significant pathological atrophy during a 3-year period, adapted from Ref. [2], and (*d*) generalized atrophy depicted affecting entire brain [3]

mechanical properties, including stiffness, softness, and friction. MRE and MRI are sensitive to localized atrophic changes, prompting extensive research to accurately quantify volumetric degeneration (brain matter shrinkage) and changing mechanical properties (shear moduli), i.e., neurodegeneration [4]. Brain MRE has been used to document the local mechanical property changes on the millimeter scale. The challenge here is to relate these mechanical property changes to the losses or alterations of neurons and glia cells (on the cell or micron-scale). This relationship can be established by employing computational mechanics. Computational mechanics play a crucial role in developing constitutive material modeling frameworks to represent the spatiotemporal patterns of atrophy evolution due to microarchitectural changes associated with human aging. For instance, Cacoilo et al. [6,7] proposed multiphysical models to predict the location and growth patterns of white matter hyperintensity in the aging brain. Detailed finite element method (FEM) analysis and multiphysics models have proven effective in identifying and simulating abnormal atrophy biomechanics [8]. These approaches can also contribute to developing brain aging and development models by incorporating multidimensionality, multi-directionality, and interindividual differences aspects [9].

Data-driven approaches, utilizing image processing of MRE/MRI scans, can be effectively integrated with multiscale and multi-physical FEM models to simulate the complex biomechanics of aging. These models can uncover critical atrophy patterns that lead to tissue softening and damage, allowing for preemptive interventions in various aging-related pathologies. With the increasing availability of public data, these models can be calibrated, optimized, and validated to serve as biomarkers for neuroimaging and neurological practitioners. This progress holds significant potential for personalized healthcare planning and intervention, as these simulations advance to provide repeatable predictions of individual aging brain biomechanics. Image processing techniques also aid in understanding region-specific brain tissue losses, which vary significantly across different brain regions [10]. Since aging impacts the entire brain structure, many researchers propose global volume measures to represent the cumulative effects of all physiological changes occurring throughout the brain. MRE/MRI scans morphologically measure in vivo changes such as brain volume loss, cortical thinning, brain white matter degradation, gyrification losses, and ventricular enlargement [1].

This study is focused on investigating age-related atrophy and softening effects on BWM in healthy aging adults. In the present work, image processing tools are deployed to process individual MRE/MRI scans and formulate a mathematical model in order to describe age-dependent BWM volume shrinkage. A novel three-dimensional (3D) micromechanical FEM has been developed in-house (Secs. 2.4 and 2.7) to simulate aging brain response to tensile loads using a tri-phasic representative volume element (RVE). Three sets of FEM are proposed to emphasize influence of volume changes, softening shear moduli (based on our previous research Agarwal et al. [11]) and finally a third ensemble of FEM cases setup to incorporate both volume shrinkage and shear moduli degradation effects to realize an aging brain response.

This research is a first of its kind attempt to develop high-order aging brain microscale FEM models to describe age dependent softening in brain matter. The image processing python code scripts are built in-house using NIBABEL libraries to read MRE/MRI scans. Data science (regression), statistical analysis, and optimization schema are then leveraged to explore various mathematical models to describe BWM volume shrinkage as a function of age (time). The derived volume shrinkage function is then used in formulating finite element (FE) codes to define volume fractions (*VF*) of axons, myelin, and extra-cellular matrix (ECM) phases in a tri phasically modeled BWM RVE. These set of FEMs were analyzed to determine effects of axon-ECM interactions, geometry, constituent material properties and phase *VFs* on brain's mechanical response. Root-mean-square deviation (RMSD) was computed between stress–strain response plots for each ensemble of aging model cases to describe degree of tissue softening brought by volume shrinkage, tissue degradation (shear moduli decay) and combination of both. Lastly, Sec. 3.5 represents a comparative

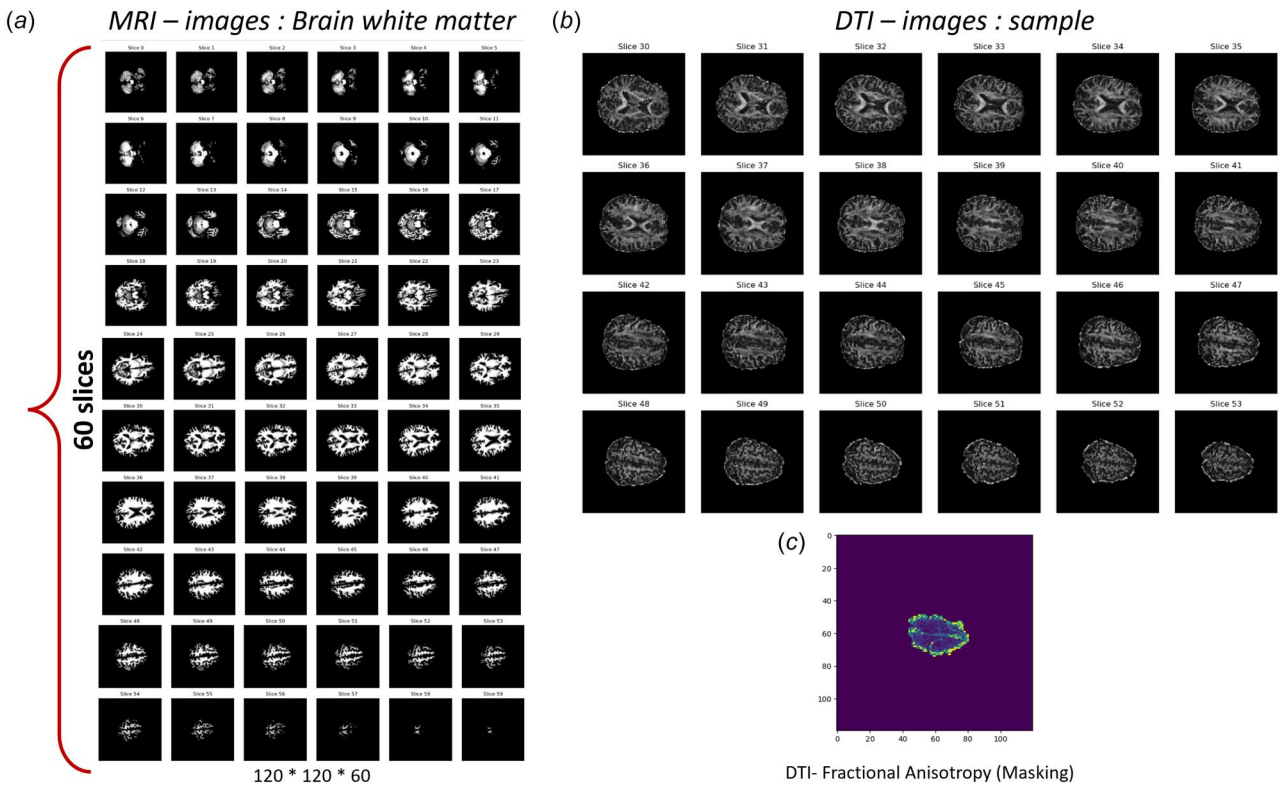

Fig. 2 (*a*) Representative figure of MRI images from one of the patient subjects chosen for this study. 60 slices of 120 × 120 resolution. The functional MRI files are stored in the NIfTi format, later processed in Python libraries (NiBabel). (*b*) DTI sample images, useful to understand integrity and connectivity in BWM, but not suitable for VF analysis since it does not provide anatomical details as MRI. (*c*) Masked images for FA measurement in DTI. All three images are for the same test subject (coded as MMMAB-0005, age 58 years). Refer Anderson et al. for more details on dataset [14].

analysis of all aging models to emphasize cumulative contributions of these atrophy factors.

2 Materials and Methods

2.1 Subjects—Data Acquisition. in vivo MRI, diffusion tensor imaging (DTI), and MRE human subject data were obtained by Dr. Georgiadis' group at Beckman Institute, Urbana, in the course of Dr. Anderson's Ph.D. work [12,13]. Brain scans of 13 healthy "young" (<35 years old) and 12 healthy "old" (55–76 years) men were acquired, in total. Informed consent was received from volunteers and local ethics committee approved the experiment protocol (refer to [13,14] for details on data availability and protection).

2.2 Magnetic Resonance Data. Magnetic Resonance Imaging (T1-weigted), DTI (30 directions), and MRE (with excitation in two directions, AP & LR) data were obtained. After postprocessing, WM/GM masks, DTI – vectors and maps, 3D complex displacement maps were provided. An isotropic inversion algorithm (NLI-MRE), allowed the extraction of viscoelastic property maps, denoted as NLI-MRE—"classic" and "converged cascade" to represent two different inversion parameters (see Fig. 2 for sample images). MRI structural data (T1-weighted) is useful to analyze morphological changes in brain. DTI produces a map of white matter tracts and connectivity by estimating the local diffusion tensor of water protons. MRE has shown lot of promise in noninvasive monitoring of changes in BWM mechanical properties. By exposing the brain to external periodic excitation, synchronized with MRI displacement-sensitive acquisition, the local displacement fields of the brain tissue in the brain are measured. Volume changes in BWM signaling atrophy can be duly assessed by MRI scans. MRE are promising biomarkers for neurodegeneration and Traumatic brain injury in healthy and aging brain [15,16].

In more detail, a total 60 MRI scans/slices are obtained for each subject and the data for only 6 subjects were used. To minimize variations in volume shrinkage calculations in whole brain parenchyma, only certain sections of magnetic resonance images are considered to minimize image edge errors. MRE scans were taken by exciting the brain in two directions: the AP (Anterior-Posterior) and LR (Left to Right) direction. In the MRE/MRI experiments—4 repeated AP- and LR-direction excitation were performed. After image analysis, key derived variables such as displacement (3D Vector field), NLIMRE—classic and WM/GM masks datasets for some processed images were obtained to aid in further imaging processing code development. We refer to Ref. [14] for further details on the raw data preprocessing steps. It is worth emphasizing here that the NLI-MRE data are obtained with an inversion scheme built on an isotropic viscoelastic constitutive model. As a result, the local viscoelastic properties differ between the two acquisitions, AP and LR.

2.3 Volume Shrinkage Analysis: Image Processing. All segmented brain volume images (60 slices) individually checked/reviewed to avoid variabilities due to residual extra-cranial components. Pathophysiological aging characteristics include neuron cell shrinking, dendritic degeneration and demyelination [1]. In this paper, image processing code is implemented on processed MRE/MRI healthy aging patient scans to formulate a mathematical model to describe age dependent BWM volume shrinkage. For this, NIBABEL libraries are used to read MRE/MRI scans and data science (regression), statistical analysis and optimization schema are deployed to fit various mathematical models to describe BWM volume shrinkage as a function of age (time). As mentioned before, each MRE/MRI patient scan

comprises of 60 layers/slices to make up the whole brain scan. Pixel based segmentation of each scan is conducted to divide it into WM and CSF/glial matrix phases. Volumetric/voxel analysis on stacked image slices then help arrive at an average volume shrinkage percentage b/w compared patient scans.

Since, we have very limited processed patient MRE data. Each of the six patient scans is compared against each other to obtain a 6 by 6 matrix volume shrinkage grid (which is an upper triangular matrix) recording relative averaged volume shrinkage percentage entries. Since we are limited by experimental data, this cross-sampling analysis method helps increase sampling space for analysis and generate data points by relative comparison of *% VF* shrinkage from one subject's data to the rest. Six patients age values are 27, 30, 32, 55, 58, and 65 years old, respectively. The 6 by 6 matrix diagonal elements are 0 (comparing each patient to itself, zero shrinkage). Hence, we are left with 15 *VF* shrinkage % unique data points. Each data point is the average volume shrinkage % value. The positive *VF* % shrinkage values in sampled data points signify loss of white matter volume from one age case to another in comparison. Meanwhile, a negative *VF* shrinkage % value would imply that WM % volume actually increased. Finally, Grid search-based regularized curve fitting and central tendency measures (statistical analysis) functions are coded in python to derive best fit mathematical model of BWM volume shrinkage as a function of age.

In the proposed volume shrinkage code, lasso and ridge regularization techniques (Tikhonov regularization) were incorporated to filter out overfitting especially for order 2 (regularized quadratic) and cubic order curves. The regularization coefficient $\lambda = 0.1$, determines the strength of regularization. To minimize the residuals, L-BFGS-B (which is a limited memory quasi-Newton method) is leveraged to evaluate the function bounds in this controlled optimization problem. After fitting and residual calculations for respective high-order *VF* function, only 80% of the data points with smallest residuals are considered to reduce impact of outliers. The models with smallest total squared residuals among considered points is chosen to describe the volume shrinkage.

Out of all possible regularized volume shrinkage function curves, see Fig. 3. Mathematical modeling suggested that $n = 3$ (cubic) order model best described the volume shrinkage as a function of age (time). This hypothesis corroborated with similar nonlinear brain

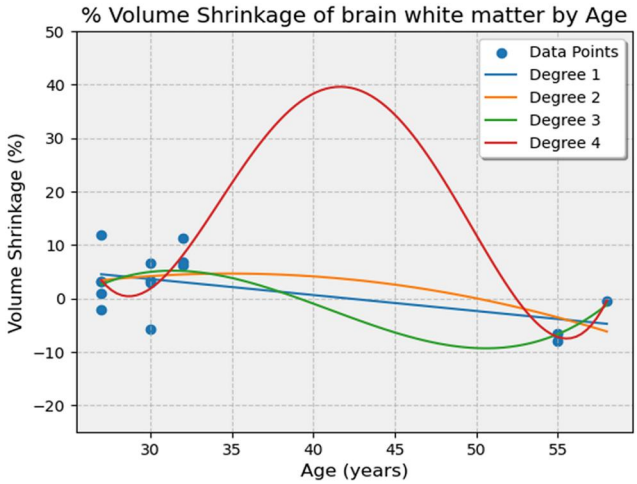

Fig. 3 Volume shrinkage (%) versus age (years) scatter plot on the MATLAB processed MRI scans of BWM for the 6 patients to obtain relative comparison points (upper triangular matrix with 15 points). Different regularization and optimization functions (grid search-based methods) implemented to fit a polynomial curve to describe high-order VF change as a function of age (time). Green curve (degree 3) resulted as the best fitting option and closed to the statistical central value. Hence, VF shrinkage function in BWM chosen as a cubic function of time (age in years). (Color version online.)

Table 1 RVE volume fractions in tri phasic BWM with age

Age (years)	Volume fraction (VF)	Axonal diameter (μm)
20	0.300	0.4370
30	0.285	0.4257
40	0.302	0.4386
50	0.328	0.4575
60	0.285	0.4258

volume and development studies suggesting similar increase in brain module and then accelerated shrinkage at old age [17]. Thus, *VF* shrinkage function equation with respect to time (t) could be described as in the following equation:

$$\mathrm{VFS}_{(t)} = 0.004,09t^3 - 0.503t^2 + 19.49t - 237.3 \tag{1}$$

2.3.1 Statistical Methods—Optimization/Regularization Methods. Along with volume shrinkage curve fitting, statistical analysis (i.e., central tendency analysis methods) such as mean and median values for MRI volumetric shrinkage analysis were also calculated in parallel for comparison to determine a median value of *VF* shrinkage over time. The median value for the entire age range was matched closely by the mean shrinkage described by cubic ($n = 3$) function for entire sampled age range, further supporting the claim to describe *VF* shrinkage function's polynomial degree by a polynomial function of degree 3.

Thus, both approaches conformed that a cubic (high-order) function could be apropos to describe nonlinear changes in brain volume over age. The findings from this study served as a critical ingredient in subsequent aging brain FEM *VF* definition step. *VF* in respective aging BWM RVEs cases (see Table 1) are a result of the image processing/data-driven *VF* analysis (Sec. 2.3).

2.4 Micromechanical Finite Element Model. To depict aging in human brain, an ensemble of microscale 3D FEMs are developed in house using Abaqus and Python scripting, see Fig. 4. RVEs is developed in series of *VFs* guided by BWM volume shrinkage analysis (Fig. 5) discussed in Sec. 2.3. The average axonal diameter for different volume fractions is enlisted in Table 1.

In the proposed 3D FEM, nonlinear Ogden Hyper-elastic (HE) constitutive material model describes the axons, myelin, and ECM material phases (Figs. 4 and 5). Ogden hyper-elastic model type is chosen to characterize BWM due to its adeptness in simulating large quasi-static strains (up to 100%) in soft rubberlike nonlinear materials.

2.5 Hyper-Elastic Material Model Component. Nonlinear hyper-elastic constitutive materials models are adept for simulating soft biological tissues [18–22]. In this study, the Ogden hyper-elastic (HE) material model has been chosen to simulate the ECM and the axons [23]. The Ogden hyper-elastic model is based on three principal stretches, λ_1, λ_2, λ_3, and *2 N* material constants. The strain energy density function, W, for the Ogden material model (Eq. (2)) in ABAQUS is formulated as [23,24]

$$W = \sum_{1}^{N} \frac{2\mu_i}{\alpha_i^2}\left(\bar{\lambda}_1^{\alpha_i} + \bar{\lambda}_2^{\alpha_i} + \bar{\lambda}_3^{\alpha_i} - 3\right) + \sum_{1}^{N} \frac{1}{D_i}(J_{el} - 1)^{2i} \tag{2}$$

where $\bar{\lambda}_i = J^{-\frac{1}{3}}\lambda_i$ and $\overline{\lambda_1\lambda_2\lambda_3} = 1$ here, J denotes a local volume change and relates to the determinant of the deformation gradient tensor F, via the right Cauchy-Green tensor $(C = F^T F)$ as $J^2 = \det(F)^2$, μ_i represents shear moduli. Meanwhile, α_i (stiffening parameter) and D_i are material parameters. In Eq. (2), J_{el} signifies elastic volume ratio. The first and the second terms represent the deviatoric and hydrostatic strain energy function components, respectively. The parameter $D_i = \frac{2}{K_0}$, allows for the inclusion of

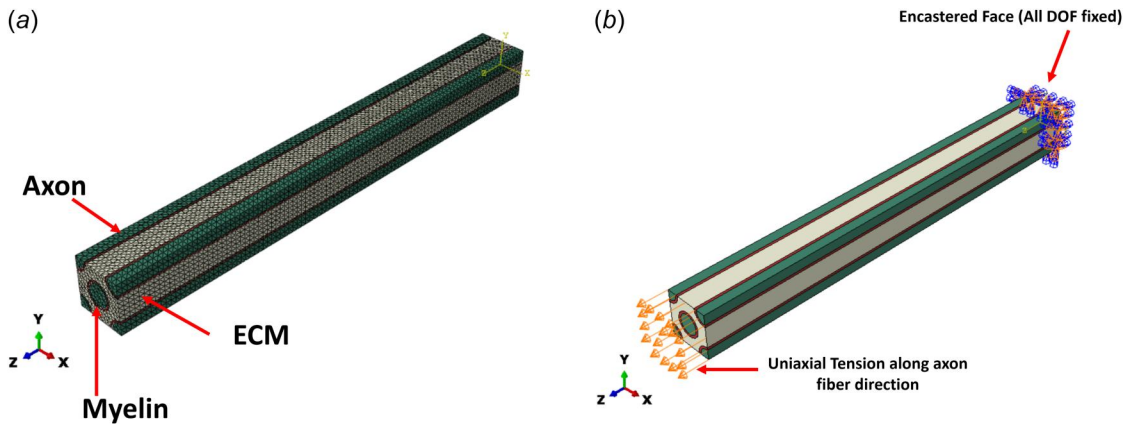

Fig. 4 (*a*) **Single RVE BWM FE model of the ECM and myelinated axons assembly packing two axon fibers, volume fraction = 0.3. The ECM (light beige), axon fibers (dark green), and myelin (dark red) phases, respectively. (*b*) Boundary conditions for single RVE. The opposite surface is fixed (displacement all DOF is set as 0, to simulate hold B.C.), while the +*z*-axis RVE face has the uni-axial tensile load applied (as shown here). Normal and tangential interactions are defined between the phases. (Color version online.)**

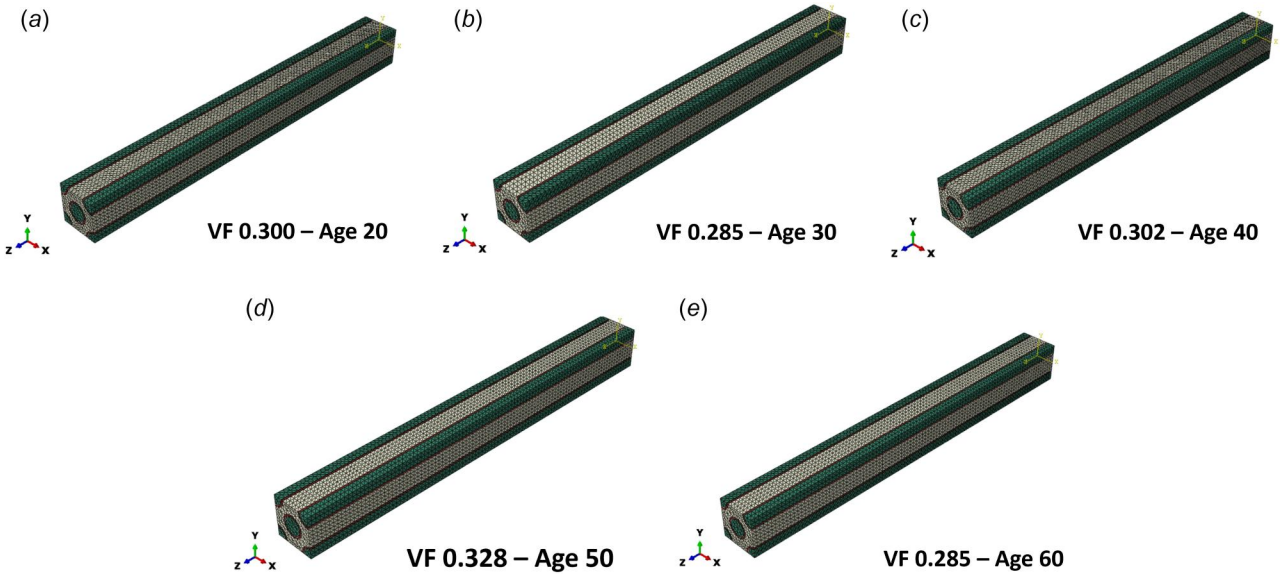

Fig. 5 (*a*)–(*e*) **Parameterization of VFs for various age depiction in micromechanical HE tri-phasic BWM RVEs. Total five cases were analyzed, ranging from Age 20–60 years. Table 1 demonstrates the VF for each RVE configuration based on image processing-based VF shrinkage calculations (Sec. 2.3).**

compressibility where K_0 is the initial bulk modulus. The same single parameter Ogden hyper-elastic material is used in this study as well [11]. Therefore, $N = 1$. Incompressibility means that $J_{el} = 1$ and is specified by setting $D_1 = 0$ in ABAQUS. ABAQUS eliminates the hydrostatic component, and the equation reduces to (Eq. (3))

$$W = \sum_{1}^{N} \frac{2\mu_i}{\alpha_i^2}\left(\bar{\lambda}_1^{\alpha_i} + \bar{\lambda}_2^{\alpha_i} + \bar{\lambda}_3^{\alpha_i} - 3\right) \tag{3}$$

In the Ogden HE models, three principal Cauchy stresses values are obtained by differentiating W with respect to λ. If an incompressible material is to be subjected under uniaxial tension ($\sigma_y = \sigma_z = 0$). Then, the resultant hyper-elastic constitutive model principal stress $\sigma_{uniaxial}$, can then be expressed as the following equation:

$$\sigma_{\text{uniaxial}} = \frac{2\mu}{\alpha}\left[\lambda^{\alpha} - \left(\frac{1}{\sqrt{\lambda}}\right)^{\alpha}\right] \tag{4}$$

In this paper, as a proof-of-concept FEM, axons are depicted as straight fibers and subjected to uniaxial tensile load. For the proposed FEM, the data for the axon and glia properties are taken from previous work and literature [16,19,20,25]. The values for shear modulus for the axons and ECM are derived from research by Wu et al. [26], α is obtained on the model proposed by Meaney [18]. The shear modulus of the ECM is specified relative to axonal shear modulus, assuming that axons are three times stiffer than ECM, as described by Arborgast and Marguile's [27]. Model

Table 2 Hyperelastic (HE) material properties summary of single-RVE FEM

Material component	μ (MPa)	D (1/ MPa)	A	Element type
Axon	2.15×10^{-3}	0	6.19	C3D4RH
ECM	8.5×10^{-4}	0	6.19	C3D4RH
Myelin	2.43×10^{-3}	0	6.19	C3D4RH

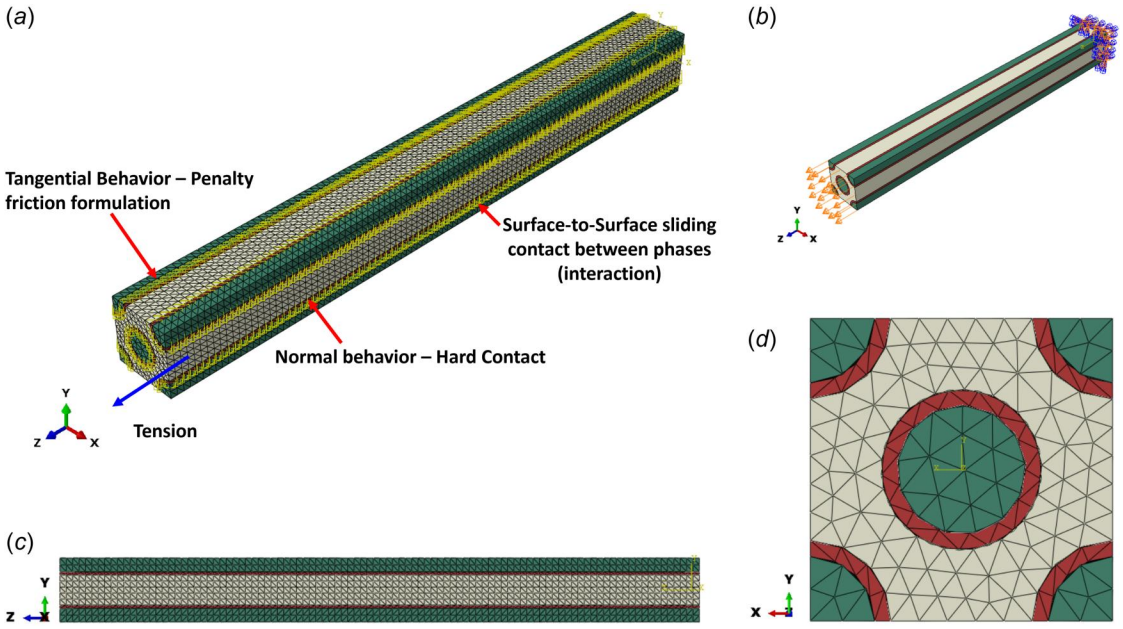

Fig. 6 (*a*) A representative RVE for tri-phasic BWM FEM setup (isoview) along with the surface-to-surface interactions defined. (*b*) FEM describing the uniaxial tensile load. (*c*) Longitudinal view of the BWM RVE. For this study, length of RVE chosen to be 10 μm, to keep it comparable with our previous aging model from 2021 [11]. (*d*) Cross section view of the BWM RVE.

incompressibility for the HE material modeling component has been deployed same as in Refs. [11,23]. Table 2 summarizes of material properties μ, D, and a, and element definition used in simulation of single RVE-HE FEM.

2.6 Aging Shear Moduli Function. The BWM soft tissues become increasingly disoriented with age, primarily due to loss of neurons and oligodendrocytes. These atrophic and aging phenomena have effect on the nonlinear hyper-elastic material properties, consequently affecting its mechanical response. In this paper, we build on the prior work done by Agarwal [11] in simulating mechanical response of an aging axon by inheriting the adjustments in material properties for defining shear moduli of HE modeled axon, myelin, and ECM phases. Detailed analytical modeling for defining hyper-elastically aging properties can be referred in Ref. [11]. Following the stated methodology, shear moduli - $\mu(t)$ can be represented as a function of age (time – t in years) as described in Eq. (5), where t_0 is age at $t = 0$ (initial condition)

$$\mu(t) = \mu(t_0)[1 - 0.008*(t - t_0)] \tag{5}$$

Note: In this paper, μ is modeled to show time-dependence decay, but other parameters (α and D_i) in the model are kept remaining constant with age. Age dependent decay in "μ" could be a higher order function (focus of our future research). Linear regression fitting technique were applied in Ref. [11] to describe a simple canonical form for FE model type I and III in this study.

2.7 Finite Element Model. In this paper, three modeling configurations are developed to realize a high-order aging brain numerical model. In model type I –*VF* variations are performed driven by image processing and optimization analytics schema to depict shrinking BWM. In type II model—a previously proposed simplified aging model by Agarwal et al. [11] is improved to serve as baseline for comparison. Finally, in type III model—volume shrinkage and shear moduli decline (as per Sec. 2.3) are incorporated to formulate a high-order micromechanical FEM.

As a proof of concept (POC), a micromechanical scale RVE geometry of dimensions ($1\,\mu m \times 1\,\mu m \times 10\,\mu m$), packing two myelinated axons in ECM material is designed to setup the finite element method (FEM) models, for depicting the three aging models (see Figs. 6(*a*)–6(*d*)). Surface-to-surface interactions are defined between the myelinated axons and ECM phases (Fig. 6(*a*)) in the triphasic BWM RVE. Myelinated axons are modeled as straight fibers. Initial volume fraction of young healthy adult is taken as 0.3 at age of 20 years (as starting point).

Please Note: The choice of RVE shape and initial *VF* are selected to keep consistency with previous aging FE model [11].

The FEM model uses a hybridized meshing framework (total elements 83,176). Hybrid Tetrahedral elements (C3D4RH) are used to discretize the three constituent phases. All elements required a linear hybrid formulation due to hyperelastic material property assignment to reproduce exact incompressibility. Definition of axon, myelin, and ECM was described as per Ogden HE material model explained in Secs. 2.5 and 2.6.

2.7.1 Finite Element Model Boundary Conditions. The tri-phasic RVEs are subjected to simple uniaxial tension (along z-direction). One of the faces is held fixed (all degree-of-freedom, displacement 0). The opposite face is subjected to tension, see Fig. 6(*b*). A uniaxial tension value is specified to simulate an ensemble of cases. The uniaxial tension is defined and solved up to 100% strain. The field output of interest is the von Mises stress (S). An implicit time integration solver technique is used in ABAQUS for computation. Contact stabilization prevents rigid body modes before contact is established between interacting surfaces of the axons and ECM.

3 Results and Discussion

Developed micromechanical aging FEMs are subjected to uniaxial tensile load to describe tissue softening behavior with aging. Micromechanical tri-phasic RVEs packing two myelinated axons (Fig. 6(*d*)) are designed as proof of concept to build three proposed aging methodologies. The FE setup, interactions and boundary conditions are applied as per Sec. 2.7, see Fig. 6. As a representative case, FEM contour plot for single-RVE is shown in Fig. 7.

3.1 Volume Shrinkage—Optimized Math Model. While MRI data for brain in several published experimental neurological studies have demonstrated atrophy in whole brain scans [5]. Both

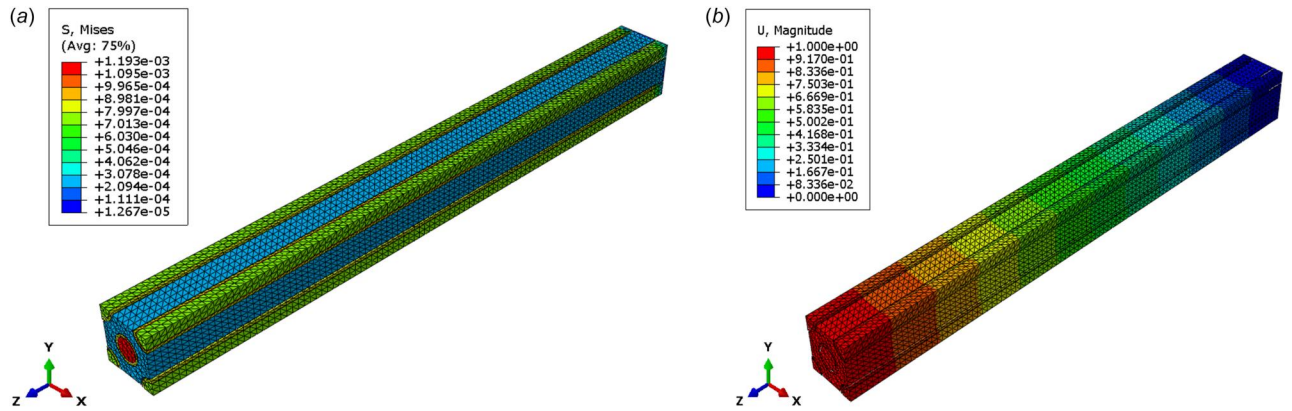

Fig. 7 Representative contour plot diagrams: (*a*) Von Mises stress contour (S) for the axons and the ECM at 10% applied stretch for single RVE FEM (along axon fiber axis—uniaxial tension load). (*b*) Total deformation (U) plot at 10% applied shear strain for Age 20—VF 0.3 BWM RVE (young adult brain case—baseline model).

Gray Matter (GM) and White Matter (WM) show shrinkage with aging. While GM's decay is more so linear, WM have been reported to have a quadratic or high-order volume loss. However, both these losses are independent of sex. A deeper mathematical treatment to this atrophy still merits lot of research. Quantitative description of such atrophy could be valuable in identifying atrophy due to diseases and differentiate normal aging atrophy from pathologically induced *VF* loss.

In this paper, MRI/MRE scans from patients were analyzed and an image processing codes were developed in Python using NIBABEL libraries to estimate a volume shrinkage function by stitching together whole brain scans (60 slices—described in Sec. 2.3). Different high order polynomial curve fitting techniques were then experimented on the matrix of volume shrinkage data on available test subjects.

Different polynomial functions were then obtained to describe the BWM atrophy. Regularization techniques were implemented to ensure overfitting functions are filtered out and a third-degree polynomial function (Fig. 3 - green curve) best represented the trend in correlation to experimental studies from other researchers. As a method of check, when statistical analysis was conducted to find a measure of central tendency (median) volume shrinkage of 3.15% was observed in the available (limited) data. Overall, a third-order polynomial (cubic) best fitted to described atrophy.

3.2 Finite Element Method Case 1—Varying Shear Moduli (Sack). Aging-related degeneration in neurons and glial cells is inevitable and experimental results from viscoelastic modeled brain by Sack et al. [28,29] suggested that this decline in whole-brain scale is predominantly linear (0.8% per annum) [29].

Leveraging this pioneering experimental research on brain atrophy based on MRE techniques have advocated brain/CNS (central nervous system) matter to be viscoelastic, but direct translation of viscoelastic properties into a hyper-elastic material type is not trivial. Hence, a cautious transfer of material properties was put forward by Agarwal et al. [11] to overcome this challenge. Refer to Sec. 2.6 for shear moduli of axon, myelin, and ECM phases for an age group of 20–60 years. In this analysis, a young healthy adult's (age 20 years) micromechanical model is progressively compared against an elderly person's (up to age of 60 years) model for the same boundary conditions (uniaxial tension case in POC FEM). A static loading simulation (tensile load in applied in z-direction) and stress versus stretch response were recorded for range of aging brain micromechanical FEM.

Discernable loss in axonal and brain matter stiffness is observed in model type I (using shear moduli decay) and constant volume fraction (Fig. 8). In each of the analyzed tri-phasic BWM RVEs, RMSD analysis is conducted to calculate variation in von-Mises

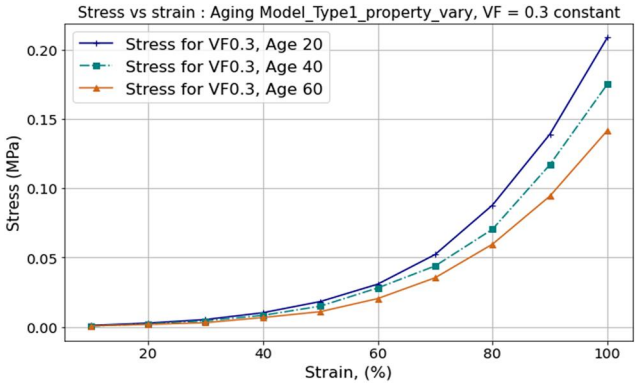

Fig. 8 Stress (σ) versus strain plot for aging model *Type I* (varying shear moduli) BWM FEM. The property variation builds on the hypothesis previously proposed by Agarwal et al. [11] and Sack et al. [29] for scope of this study, three age cases are plotted (ages: 20, 40, and 60). RMSD analysis clearly indicated tissue softening with age. RMSD b/w curves for Ages 20 and 60 is 0.0278.

profiles for varying ages. RMSD is defined as $\sqrt{\frac{\left(f(x_i)-g(x_i)\right)^2}{N}}$ for curves $f(x)$, $g(x)$, and N being number of points x_i at which curves are compared. RMSD b/w von Mises (S) for BWM RVEs (model type 1) b/w age 20 and age 40 curve is found to be 0.0142. Meanwhile, RMSD b/w age 40 and age 60 curves (Fig. 8) is calculated as 0.0138 showing a clear progressive brain tissue softening and atrophy with aging. RMSD b/w age 20 (youngest) and age 60 (oldest test case) stress curve is 0.0278.

3.3 Finite Element Method Case 2—Varying Volume Fraction. Using the approach 1 (see Sec. 3.2), a steady decline in max. stress is noticed indicating a gradual BWM softening. This was characterized in first installment of the research by Agarwal et al. [11] in 2021 on the oligodendrocyte FEM setup. But aging in human brain manifests much complex biomechanics then sheer change of shear moduli over time. Hence, variability in *VF* is explored to describe this high-order atrophy. In model type II, an ensemble of cases is run to characterize stress versus stretch response for varying *VF* (determined by the data-driven regularized curve fitting as explained in Sec. 2.3).

RMSD b/w von Mises (S) for BWM RVEs (model type II) b/w age 20 and age 40 curve is found to be 0.0423. Meanwhile, RMSD b/w age 40 and age 60 curves (Fig. 9) is calculated as 0.003. RMSD b/w curves for Age 20 and Age 50 is 0.0089. While RMSD between Age

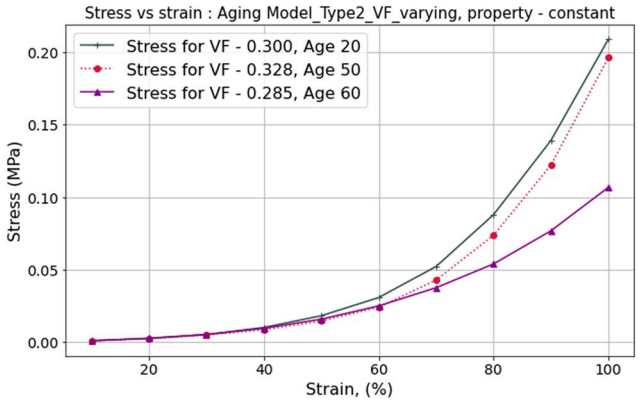

Fig. 9 Stress (σ) versus strain plot for aging model *Type II* (varying volume fractions) BWM FEM. The VF variation is guided by the shrinkage function proposed in Sec. 2.3. In contrast to type I, this model showed modest increase in stiffness from age 40 to 50, but overall, WM atrophy affects dominated a softening trend with age, as seen in presented plots.

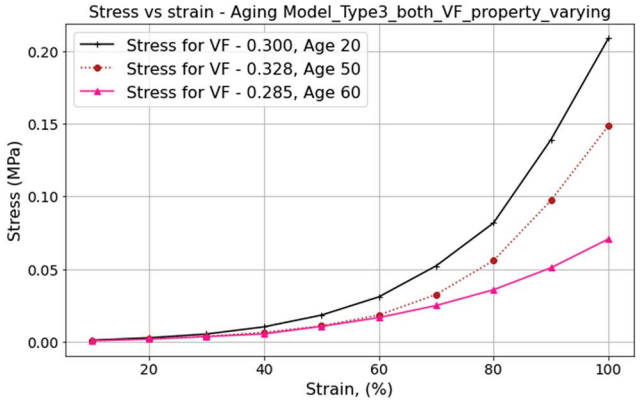

Fig. 10 Stress (σ) versus strain plot for aging model *Type III*—varying both volume fractions and shear moduli (property) in the BWM FEM RVEs. As opposed to model Type II, greater tissue softening observed with age. RMSD b/w Age 20 and Age 60 curves increased to 0.0547 by 38.13% compared to model Type II RMSD (0.0396 b/w the same two cases).

50 and 60 is 0.0323. RMSD b/w age 20 (youngest) and age 60 (oldest test case) stress curve is 0.0396. There was 42% increase in RMSD noticed between 20 versus 60 age plots in Model II compared to Model I, showing nonlinear softening trend due to loss of white matter tissues with age.

3.4 Finite Element Method Case 3—Varying Shear Modulus and Volume Fractions. As a proof of concept, a third aging brain model is then proposed which incorporates the variation in brain volume (shrinkage) and shear moduli variation to capture the tissue softening and atrophy with age. In model type III, RVEs are analyzed by varying the *VF* using the developed shrinkage function and the shear moduli variation is considered to follow the trend described in Sec. 2.6. Total 5 age cases are modeled, ranging from 20 to 60 years. For the scope of this paper, stress versus strain plots is shown for only three age cases, see Fig. 10.

RMSD b/w von Mises (S) for BWM RVEs (model type III) b/w age 20 and age 40 curve is found to be 0.0484. Meanwhile, RMSD b/w age 40 and age 60 curves (Fig. 10) is calculated as 0.0065. RMSD b/w age 20 and 50 curves are 0.0258 and RMSD b/w the von-Mises stress plots age 50 and 60 is 0.0294. RMSD b/w age 20 (youngest) and age 60 (oldest test case) stress curve is 0.0547. This

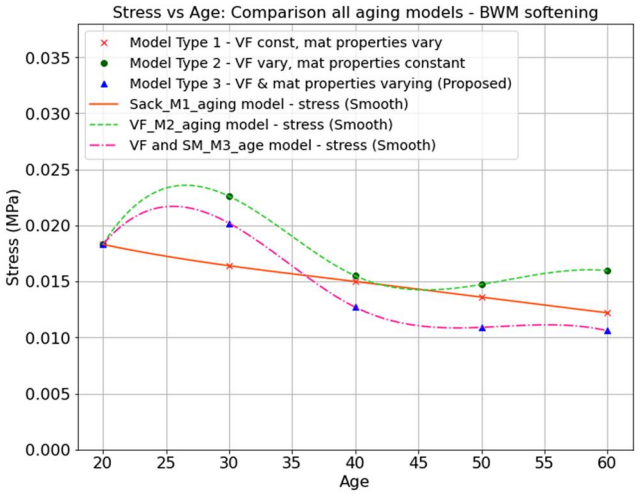

Fig. 11 Stress (σ) versus shear strain % plots of aging brain RVE FEMs for all three model types. In corroboration with our previous studies, model Type I (brown curve) showed a linear decay in tissue stiffness but incorporating volume change (atrophy) and property decay (shear moduli softening) parameters together in model Type III (magenta color) led to a nonlinear tissue response demonstrating a high-order WM tissue softening with age. (Color version online.)

RMSD value is 38% more b/w same corresponding cases (Age 20 versus Age 60 plot), verifying greatest extent of BWM softening amongst all proposed models.

3.5 Comparison of Aging Models—Softening. Using the approach 1 (Sec. 3.2), a steady decline in max. stress is noticed indicating a gradual BWM softening. This was characterized in first installment of the aging brain research by Agarwal et al. [11] on the oligodendrocyte FEM setup. But, as explained, aging behavior are complex and often a culmination of several factors. In this section, all three models are compared, see Fig. 11.

Root-mean-square deviation analysis was conducted between all proposed and analyzed aging brain computational models. RMSD b/w method 1 (*varying shear moduli*—Brown curve) and Method 2 (*varying volume fractions*—green curve) is 0.0032. RMSD b/w method 1 and method 3 (*varying both VF and shear moduli* together—magenta color) is 0.00243. Finally, RMSD b/w Method 2 and Method 3 observed to be 0.0034. As demonstrated in another similar animal FE aging brain study, a very similar high-order stress versus age variation is noticed , i.e., gradual stiffening at adult and accelerated softening with old age [17]. This research help verified that incorporating atrophy (*VF*) affects in modes of BWM shrinkage and reducing shear moduli (softening), a high-order brain matter neurodegeneration can be clearly described (Fig. 11).

3.6 Model Limitations and Assumptions. The proposed FEM has few limitations. First, the model approximated pure nonaffine boundary conditions for entire stretch, even though physiologically axons tend to exhibit more of transitional kinematics [11]. For aging brain analysis, impact of degradation on α and K was not factored in the Ogden HE modeled BWM [11]. In future, high-order Ogden HE material models would be coded in FORTRAN (UMAT) [30] to define aging BWM phases. Other ensemble load cases such as shear and twist can be explored to characterize aging brain response [31].

The proposed data-driven paradigm for calculating a high-order volume shrinkage in BWM is heavily dependent on data available at disposal for analysis. As more diverse MRI/MRE data (i.e., across all age groups) become available, it would aid in attaining robust volume shrinkage fitting functions. Also, in the current study, only shrinkage related the atrophy of the healthy brain was considered. Such shrinkages can be caused by brain injuries, biochemical factors (substance abuse, alcohol consumption), chronic habits, dementia,

or other neurodegenerative conditions. Sampling datapoints from such patient groups are also necessary to benchmark atrophy caused by healthy and other pathologies. Nonlinear decay characteristics could be incorporated in the study of aging brain matter's response if verified time decay functions for "α" and "K" parameters in the Ogden HE material model can be obtained from experiments. In presented simulations, damage initiation and evolution were not discussed either.

4 Conclusions

In this research, three aging brain models are presented. An ensemble of uniaxial tensile load simulation cases is experimented for varying RVE configurations (Fig. 5). Resultant stress vs. strain plots clearly showed that pertinent cerebral damage due to aging is dependent on BWM micro-architecture (geometry), *VF*, loading direction and current state of the shear moduli (impact of aging, injury, or atrophy), i.e., model type III (proposed aging model). Analytical framework developed for BWM Volume fraction shrinkage function guided by image processing and optimization schema showed clear high-order atrophy (Fig. 11), in line with previous studies [5]. Comprehensive modeling of an aging brain's biomechanics could be very useful in application such as preventive health care management and surgical simulation, protective head gear design and tissue-surgical tool interactions.

Starting from multi-excitation MRE/MRI experimental data [13], the employment of distinct isotropic material properties in well-ordered WM tracts helped determine BWM FEM constituent phase properties (shear moduli). These shear moduli were then varied along with fiber *VF* in model type III to attain a high-order aging brain stiffness and tissue softening characterization. The models also emphasized contributions from highly anisotropic nature of BWM to gradual neurodegeneration. Understand these age-dependent factors in brain also affect injury risk indicators. In the future, devising 3D FE BWM model incorporating damage accumulation and fatigue behavior would provide a detailed understanding of structural response of young, aging, or injured axons to external loads [11].

Acknowledgment

The opinions, findings, conclusions, or recommendations expressed are those of the author(s) and do not necessarily reflect the views of the National Science Foundation.

Funding Data

- NSF (Grant Nos. CMMI-1436743, CMMI-1437113, CMMI-1762774, and CMMI-1763005; Funder ID: 10.13039/100000001).

Data Availability Statement

The datasets generated and supporting the findings of this article are obtainable from the corresponding author upon reasonable request.

Nomenclature

C = Cauchy-Green deformation tensor (right)
F = deformation gradient tensor
W = Ogden strain-energy density function
α = alpha
λ = principal stretches
μ = shear moduli (hyper-elastic: Ogden model)
σ = principal stress
τ = shear stress
AP = anterior-posterior
DTI = diffusion tensor imaging
LR = left-right
MRE = magnetic resonance elastography
MRI = magnetic resonance imaging

References

[1] Blinkouskaya, Y., Caçoilo, A., Gollamudi, T., Jalalian, S., and Weickenmeier, J., 2021, "Brain Aging Mechanisms With Mechanical Manifestations," Mech. Ageing Dev., **200**, p. 111575.
[2] Blinkouskaya, Y., and Weickenmeier, J., 2021, "Brain Shape Changes Associated With Cerebral Atrophy in Healthy Aging and Alzheimer's Disease," Front. Mech. Eng., **7**, p. 705653.
[3] Rana Ahmed, A. C., 2023, "Cerebral Atrophy Overview, Causes & Diagnosis," Blog and Tutorial Series, Mountain View, CA, accessed Nov. 21, 2023, https://study.com/academy/lesson/cerebellar-atrophy-causes-symptoms.html
[4] Weickenmeier, J., 2023, "Exploring the Multiphysics of the Brain During Development, Aging, and in Neurological Diseases," Brain Multiphys., **4**, p. 100068.
[5] Ge, Y., Grossman, R. I., Babb, J. S., Rabin, M. L., Mannon, L. J., and Kolson, D. L., 2002, "Age-Related Total Gray Matter and White Matter Changes in Normal Adult Brain. Part I: Volumetric MR Imaging Analysis," Am. J. Neuroradiol., **23**(8), pp. 1327–1333.
[6] Caçoilo, A., Dortdivanlioglu, B., Rusinek, H., and Weickenmeier, J., 2023, "A Multiphysics Model to Predict Periventricular White Matter Hyperintensity Growth During Healthy Brain Aging," Brain Multiphys., **5**, p. 100072.
[7] Caçoilo, A., Rusinek, H., and Weickenmeier, J., 2022, "3D Finite-Element Brain Modeling of Lateral Ventricular Wall Loading to Rationalize Periventricular White Matter Hyperintensity Locations," Eng. Comput., **38**(5), pp. 3939–3955.
[8] Agarwal, M., Pasupathy, P., Wu, X., Recchia, S. S., and Pelegri, A. A., 2024, "Multiscale Computational and Artificial Intelligence Models of Linear and Nonlinear Composites: A Review," Small Sci., **4**(5), p. 2300185.
[9] Ziegler, G., Dahnke, R., Gaser, C., and Initiative, A., 2012, "Models of the Aging Brain Structure and Individual Decline," Front. Neuroinf., **6**, p. 3.
[10] Coffey, C., Wilkinson, W., Parashos, L., Soady, S., Sullivan, R., Patterson, L., Figiel, G., Webb, M., Spritzer, C., and Djang, W., 1992, "Quantitative Cerebral Anatomy of the Aging Human Brain: A Cross-Sectional Study Using Magnetic Resonance Imaging," Neurology, **42**(3), p. 527.
[11] Agarwal, M., Pasupathy, P., De Simone, R., and Pelegri, A. A., 2021, "Oligodendrocyte Tethering Effect on Hyperelastic 3D Response of Injured Axons in Brain White Matter," ASME Paper No. IMECE2021-73376.
[12] Gallo, N. R., 2020, "Variation of In Vivo Anisotropic MRE Metrics in Corpus Callosum: Effect of Aging," Proceedings of the International Society for Magnetic Resonance in Medicine Scientific Meeting and Exhibition, Virtual Conference, Aug. 8–14, p. 28.
[13] Anderson, A. T., 2018, "Magnetic Resonance Elastography and Nonlinear Inversion Problem in the Aging Brain," Ph.D. dissertation, University of Illinois at Urbana-Champaign, Champaign, IL.
[14] Anderson, A. T., Van Houten, E. E., McGarry, M. D., Paulsen, K. D., Holtrop, J. L., Sutton, B. P., Georgiadis, J. G., and Johnson, C. L., 2016, "Observation of Direction-Dependent Mechanical Properties in the Human Brain With Multi-Excitation MR Elastography," J. Mech. Behav. Biomed. Mater., **59**, pp. 538–546.
[15] Bayly, P. V., Alshareef, A., Knutsen, A. K., Upadhyay, K., Okamoto, R. J., Carass, A., Butman, J. A., et al., 2021, "MR Imaging of Human Brain Mechanics in Vivo: New Measurements to Facilitate the Development of Computational Models of Brain Injury," Ann. Biomed. Eng., **49**(10), pp. 2677–2692.
[16] Agarwal, M., Pasupathy, P., and Pelegri, A. A., 2022, "Oligodendrocyte Tethering Effect on Hyperelastic 3D Response of Axons in White Matter," J. Mech. Behav. Biomed. Mater., **134**, p. 105394.
[17] Antona-Makoshi, J., Eliasson, E., Davidsson, J., Ejima, S., and Ono, K., 2015, "Effect of Aging on Brain Injury Prediction in Rotational Head Trauma—a Parameter Study With a Rat Finite Element Model," Traffic Inj. Prev., **16**(sup1), pp. S91–S99.
[18] Meaney, D. F., 2003, "Relationship Between Structural Modeling and Hyperelastic Material Behavior: Application to CNS White Matter," Biomech. Model. Mechanobiol., **1**(4), pp. 279–293.
[19] Pan, Y., Sullivan, D., Shreiber, D. I., and Pelegri, A. A., 2013, "Finite Element Modeling of CNS White Matter Kinematics: Use of a 3D RVE to Determine Material Properties," Front. Bioeng. Biotechnol., **1**, p. 19.
[20] Pan, Y., Shreiber, D. I., and Pelegri, A. A., 2011, "A Transition Model for Finite Element Simulation of Kinematics of Central Nervous System White Matter," IEEE Trans. Biomed. Eng., **58**(12), pp. 3443–3446.
[21] Brooks, T., Choi, J. E., Garnich, M., Hammer, N., Waddell, J. N., Duncan, W., and Jermy, M., 2018, "Finite Element Models and Material Data for Analysis of Infant Head Impacts," Heliyon, **4**(12), p. e01010.
[22] Singh, S., Pelegri, A. A., and Shreiber, D. I., 2015, "Characterization of the Three-Dimensional Kinematic Behavior of Axons in Central Nervous System White Matter," Biomech. Model. Mechanobiol., **14**(6), pp. 1303–1315.
[23] Pasupathy, P., De Simone, R., and Pelegri, A. A., 2020, "Numerical Simulation of Stress States in White Matter Via a Continuum Model of 3D Axons Tethered to Glia," ASME Paper No. IMECE2020-24667.
[24] ABAQUS, User's Manual, and Standard User's Manual, 2005, "Hibbitt, Karlsson, and Sorensen," Inc V5 8.
[25] Agarwal, M., 2022, "Numerical Simulation of Stress States to Evaluate Oligodendrocyte Tethering Effect on Hyperelastic 3D Response of Injured Axons in Brain White Matter." Master's thesis, Rutgers, The State University of New Jersey, School of Graduate Studies.

[26] Wu, X., Georgiadis, J. G., and Pelegri, A. A., 2019, "Brain White Matter Model of Orthotropic Viscoelastic Properties in Frequency Domain," ASME Paper No. IMECE2019-12182.
[27] Arbogast, K. B., and Margulies, S. S., 1998, "Material Characterization of the Brainstem From Oscillatory Shear Tests," J. Biomech., **31**(9), pp. 801–807.
[28] Sack, I., Streitberger, K.-J., Krefting, D., Paul, F., and Braun, J., 2011, "The Influence of Physiological Aging and Atrophy on Brain Viscoelastic Properties in Humans," PloS One, **6**(9), p. e23451.
[29] Sack, I., Beierbach, B., Wuerfel, J., Klatt, D., Hamhaber, U., Papazoglou, S., Martus, P., and Braun, J., 2009, "The Impact of Aging and Gender on Brain Viscoelasticity," Neuroimage, **46**(3), pp. 652–657.
[30] Connolly, S. J., Mackenzie, D., and Gorash, Y., 2019, "Isotropic Hyperelasticity in Principal Stretches: Explicit Elasticity Tensors and Numerical Implementation," Comput. Mech., **64**(5), pp. 1273–1288.
[31] Agarwal, M., and Pelegri, A. A., 2024, "An Ogden Hyperelastic 3D Micromechanical Model to Depict Poynting Effect in Brain White Matter," Heliyon, **10**(3), p. e25379.